

**ATAL BIHARI VAJPAYEE - INDIAN INSTITUTE OF INFORMATION
TECHNOLOGY AND MANAGEMENT GWALIOR - 474015**



विश्वजीवनामृतं ज्ञानम्

Machine Learning Knowledge Based Models for GNR Interconnects

A Mini Project report,
Submitted By:

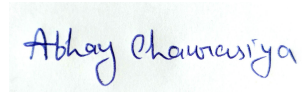
Abhay Chaurasiya(2018IMT-005)

Under the supervision of:

Dr. Somesh Kumar

CANDIDATES DECLARATION

I hereby certify that the work, which is being presented in the report, entitled **Machine Learning Knowledge Based Models for GNR Interconnects**, in complete fulfillment of the requirement for the course-Mini Project(ITIT 3203) submitted to the institution is an authentic record of our own work carried out during the period February 2021 to May 2021 under the supervision of **Prof. Somesh Kumar**. We also cited the reference about the text(s)/figure(s)/table(s) from where they have been taken.



Date: 24-05-2021

Signatures of the Candidates

This is to certify that the above statement made by the candidates is correct to the best of my knowledge.



Date: 24-05-2021

Signatures of the Research Supervisors

ACKNOWLEDGEMENTS

I am highly indebted to **Dr. Somesh Kumar Dahiya**, and am obliged for giving me the autonomy of functioning and experimenting with ideas. I would like to take this opportunity to express my profound gratitude to him not only for his academic guidance but also for his personal interest in my project and constant support coupled with confidence boosting and motivating sessions which proved very fruitful and were instrumental in infusing self-assurance and trust within me. The nurturing and blossoming of the present work is mainly due to his valuable guidance, suggestions, astute judgment, constructive criticism and an eye for perfection. My mentor always answered the myriad of my doubts with smiling graciousness and prodigious patience, never letting me feel that I am novices by always lending an ear to my views, appreciating and improving them and by giving me a free hand in my project. It's only because of his overwhelming interest and helpful attitude, the present work has attained the stage it has. Finally, I am grateful to my Institution and colleagues whose constant encouragement served to renew my spirit, refocus my attention and energy and helped me in carrying out this work.

(Abhay Chaurasiya)

CONTENTS

Abstract	4
Background Information/Motivation	4
Literature Survey	5
Project Objectives	6
Methodology	6
System Architecture	6
Block Diagram	8
Implementation Details	10
Techniques used	12
Testing Details	14
Result and Discussion	14
Conclusion	18
Future Work	18
References	18

Abstract

With the scaling down of integrated circuits (ICs) into nanometer sizes, new challenges have emerged for conventional Cu interconnects. These Problems are due to surface scattering, heat dissipation, electromigration, grain boundaries, and current capacity issues . Carbon nanomaterials like graphene nanoribbons (GNRs) and carbon nanotubes (CNTs) have attracted a better research interest as candidates for replacing Cu nanowire interconnects in advanced ICs. Graphene nanoribbons (GNRs) are considered as a destined interconnect material. Multilayer graphene nanoribbon MLG NR interconnects performance are better than Cu counterparts with the same dimensions both in terms of bandwidth and time delay.

In this Project we made various Machine Learning Models for predicting MFP due to scattering by edge roughness at given wavelength , predicting MFP due to scattering by edge roughness at given fermi energy ,predicting the effective MFP of electrons in GNR at given wavelength ,predicting the effective MFP of electrons in GNR at given fermi energy , predicting the number of layers in MLG NR at given thickness, predicting scattering resistance , lumped resistance and quantum resistance resulting in the prediction of the total resistance. It takes immense hard work to compute the total resistance from the given values and knowing the value of resistance is fundamental to the computation of many other factors , for this purpose we have come up with machine learning models to compute various parameters.

Background Information/Motivation

IC performance is dominated by Delays in interconnects, power consumption and bandwidth because of enlargement in size of chip and limiting in its minimum feature size, despite new materials such as Cu (low-k dielectric). Thus chip performance is limited sharply without a pattern move from present interconnect architecture being introduced. In 3-D ICs the vertical interconnects of multiple active Si layers are promising techniques. If long horizontal interconnects can be replaced by short vertical inter-layer interconnects , improvement in performance and reduction in wire-limited chip area can be achieved with 3-D ICs. Due to the increase in power density in 3-D circuits we are also addressing the thermal concern.

In electronic devices Cu is used instead of aluminium due to its higher thermal dissipation. Whereas, Cu is difficult to expel, stamp or machine, therefore it is a more

common process powder metallurgy technique. Pure sintered Cu has lower thermal conductivity (300-330 W/m.K) than the monocrystal pure copper (401 W/m.K), due to the existence of grain boundaries and defects in polycrystals structures. Due to its high exceptional strength, low coefficient of thermal expansion and ultra-high thermal conductivity(3000-6000W/m.K) Carbon Nanotube(CNT) is one of the most promising materials in the field of advanced materials. The avg thermal conductivity of multilayer CNT is 3000W/m.K, which is approximately 8 times higher than that of pure Cu(401W/m.K). So adding a small number of CNTs to the Cu matrix is expected to contribute strongly to improving the overall thermal conductivity which in turn can be used as a heat dissipator in advanced electronics devices.

On the basis of edge geometry there are three types of GNRs available . They are:

- Armchair (AGNR)
- Zigzag (ZGNR)
- Chiral (CGNR)

33% of AGNRs are semiconducting with respect to the number of carbon atoms present in AGNR width and also entire ZGNRs are metallic.

Literature Survey

The on chip GNR interconnects have been examined as one of the most stimulating areas in wide-ranging scale integration for the last several years. In nano size, the interconnect delay becomes more obvious than gate delay. With the help of Properties of the interconnects we will best describe the reliability and the on chip performance instead of the transistors. The resistivity and reliability are becoming two more serious issues for selecting the best interconnect materials. Due to the extraordinary electrical and their other properties, graphene becomes a dependable contender for next generation interconnects. From the research it has been shown that the configuration of the ICs introduces inductive, resistive and capacitive exploitative components.

Graphene has the high current density with lowest resistivity ,high electron mobility and large mean free path. From the research it has been concluded that narrow width graphene nanoribbon (GNR) or graphene sheet is the most acceptable interconnect material. Whereas, the electrical property of GNR can be changed by changing geometric configuration to a minor range to differentiate the modesty of graphene film. The electrical resistance of SLGNR is relatively high as compared to Cu.

Project Objectives

The project objectives are as follow:

- Creating a machine learning model to predict the number of layers in GNR at given thickness.
- Developing a machine learning model to predict MFP due to scattering by edge roughness at given wavelength
- Developing a machine learning model to predict MFP due to scattering by edge roughness at given fermi energy
- Developing a machine learning model to predict the effective MFP of electrons in GNR at given wavelength
- Developing a machine learning model to predict the effective MFP of electrons in GNR at given fermi energy
- Developing a machine learning model to predict scattering resistance,lumped resistance and quantum resistance resulting in the prediction of the total resistance.

Methodology

System Architecture

In a MLGNR, the space between ground plane and MLGNR is filled with an insulator, the permittivity of which is considered to be $\epsilon_r = 3.9$. The total number of GNR layers depends on the MLGNR thickness (T) and interlayer spacing (δ) between adjacent MLGNRs as follows:
$$N_{layer} = 1 + Integer\left(\frac{t}{\delta}\right) \quad (1)$$

where δ is two layer distance which is considered as 0.34nm.

The lumped resistance R_{lu} consists of the imperfect metal–MLGNR contact resistance (R_{mc}) and quantum resistance (R_q) due to the quantum confinement of carriers across the interconnect width. The lumped resistance is assumed to be equally divided between the two contacts as follows:

$$R_{lu} = (R_{mc} + R_q)/2 \quad (2)$$

where

$R_{mc} = 6.45/N_{ch}$ k Ω for Metal - SLGNR contact,

$R_{mc} = 6.45/(N_{ch} * N_{layer})$ for Metal - MLGNR contact,

$R_q = 12.9/N_{ch} \text{ k}\Omega$ for Metal - SLGNR contact,
 $R_q = 12.9/(N_{ch} * N_{layer}) \text{ k}\Omega$ for Metal - MLGNR contact.

The scattering resistance is given as :

$$R_s = 12.9/(N_{ch} * N_{layer} * \lambda_{eff}) \quad (3)$$

Where to calculate λ_{eff} , we use Matthiessen's rule according to which the effective MFP for the nth sub-band $\lambda_{eff,n}$ can be written as

$$\frac{1}{\lambda_{eff,n}} = \frac{1}{\lambda_d} + \frac{1}{\lambda_{pn}} + \frac{1}{\lambda_{er,n}} + \frac{1}{\lambda_{sr}} \quad (4)$$

In which λ_d is the MFP due to crystal defect and impurities which is taken as 1um,
 $\lambda_{p,n}$ is the MFP due to electron phonon scattering which is 70um and is ignored in calculations as it is very much higher in comparison to others,

λ_{sr} is the MFP due to surface roughness scattering which is given as $\lambda_{sr} = c/y_{sr}^4$ where $c = 2.07 * 10^9$ and y_{sr} = surface roughness which is taken as 20pm in our calculations,

$\lambda_{er,n}$ is given by

$$\lambda_{er,n} = \frac{W}{p} \sqrt{\left(\frac{2WE_f}{nhv_f}\right)^2 - 1} \quad (5)$$

where p denotes the backscattering probability at the edges, that is p = 0 corresponds to GNRs with perfect edges, while $0 < p \leq 1$ applies to GNRs with rough edges,

W is the wavelength in nm,

n=3

h=Planck's constant in eV/Hz

$v_f = 8 * 10^9$ m/s

E_f = fermi energy in eV.

Block diagram/ Figures Used:

- Fig.1 shows an MLGNR of width W and thickness T placed at distant d over a ground plane. The space between ground plane and MLGNR is filled with an insulator, the permittivity of which is considered to be $r = 3.9$.

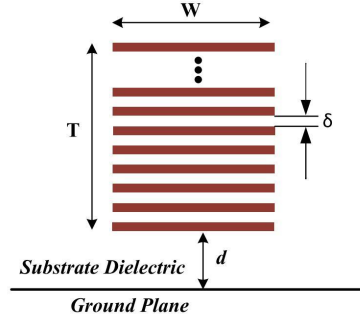


Fig. 1. Geometry of the MLGNR-dielectric-ground system.

- Fig. 2 shows the ESC model of a typical MLGNR interconnect with length L . The lumped resistance R_{lu} consists of the imperfect metal–MLGNR contact resistance (R_{mc}) and quantum resistance (R_q) due to the quantum confinement of carriers across the interconnect width.

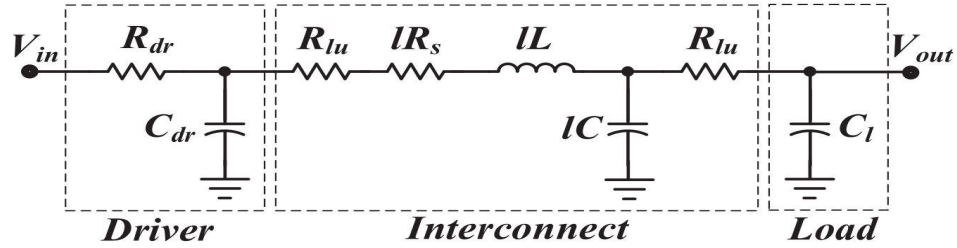


Fig. 2. ESC circuit model of MLGNR interconnect.

- Fig. 3 shows Geometries of (a) SLGNR and (b) MLGNR interconnect with side contacts over a ground plane. The interval spacing between adjacent layers in the MLGNR is $\delta = 0.34$ nm, i.e., the Van der Waals gap.

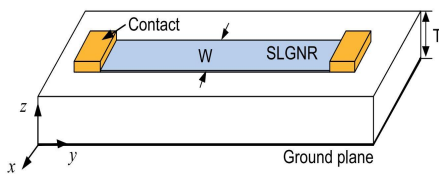


Fig.3.(a) SLGNR Interconnect

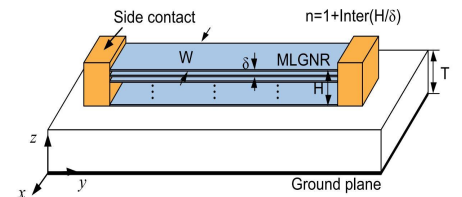


Fig.3.(b) MLGNR Interconnect

□ Fig.4 shows the Equivalent single conductor model of MLGNR interconnect.

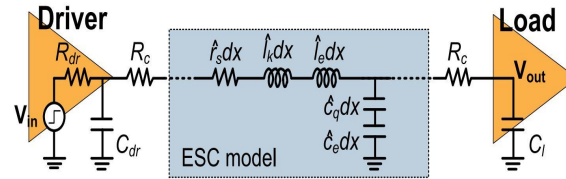
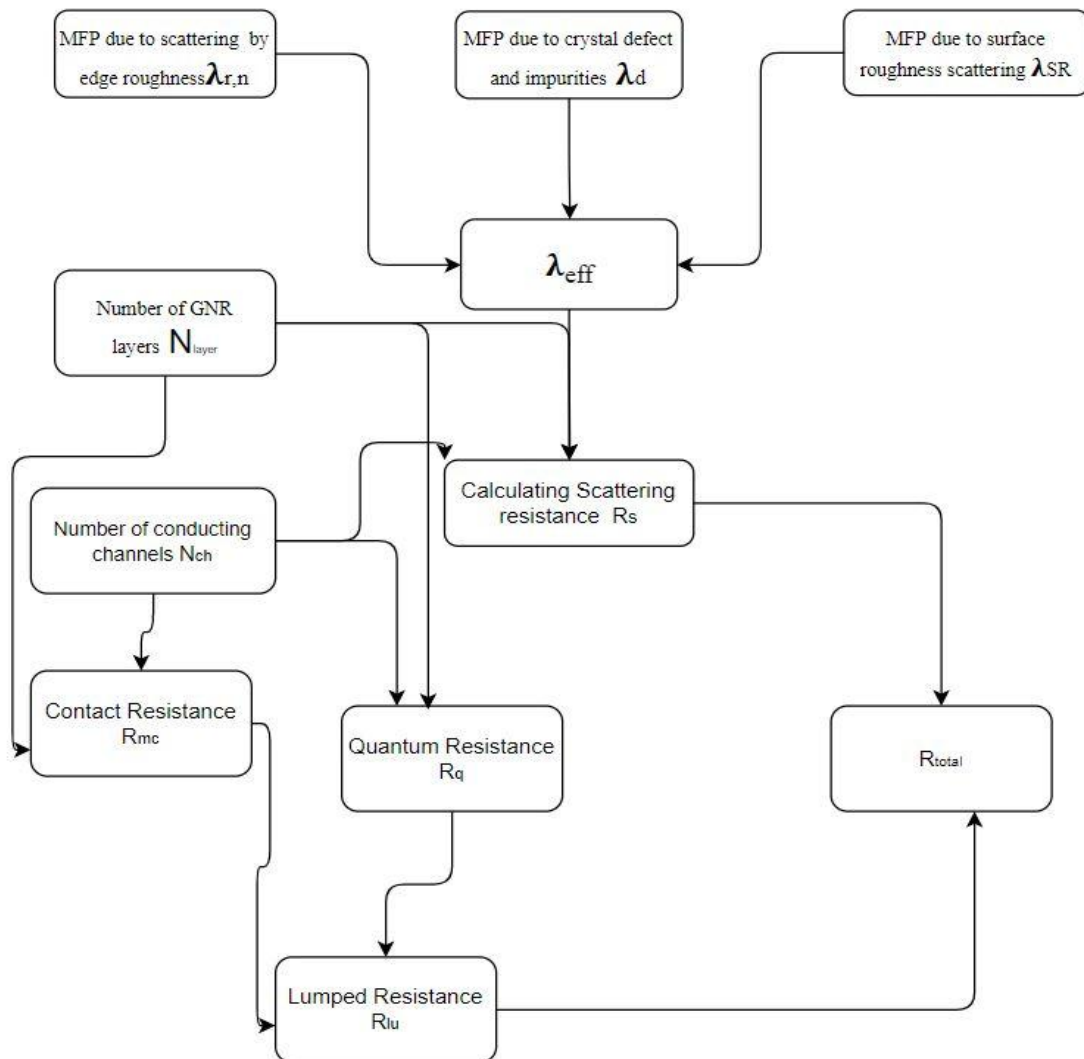


Fig. 4. ESC model of MLGNR interconnect.

□ Flow Chart of the work.



Implementation details

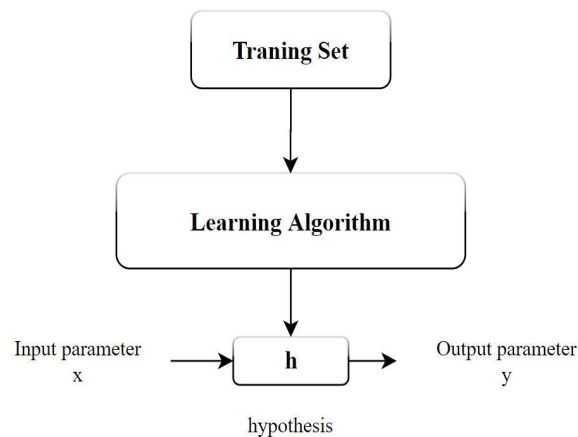
Tools Used

We have used a number of programming and machine learning tools for our project. Some of them are:

- Programming Language - Python
- Libraries used:
 - numpy for creating arrays and working in them.
 - pandas for reading and creating csv files and working on dataframes.
 - sklearn for making use of some predefined models like linear regression and polynomial regression.
 - matplotlib for plotting various graphs and contours.
 - SciPy for extracting the values of several scientific constants used in our project.
- Software for plotting graphs- Origin.
- Platform used for creating models-Jupyter Notebook and Google Collab Notebook.

Setup

We have used the following setup while creating our each model for each equation:



For each equation we have used some hypothesis .

- For equation

$$N_{layer} = 1 + Integer\left(\frac{t}{\delta}\right) \quad (6)$$

We have used linear regression model and hypothesis as $\mathbf{h} = \boldsymbol{\theta}_0 + \boldsymbol{\theta}_1 * \mathbf{x}$ where our model is trained to learn the value of $\boldsymbol{\theta}_0$ and $\boldsymbol{\theta}_1$.

How do we train our model ?

- We provide the values of t as x to our model and N_{layer} as y to our model.
- Model tries to learn the value of $\boldsymbol{\theta}_0$ and $\boldsymbol{\theta}_1$.
- Model learns the value of $\boldsymbol{\theta}_0$ and $\boldsymbol{\theta}_1$ and use it to predict the value of N_{layer} .
- We plot the graph of N_{layer} vs t and then between N_{layer} predicted and t to know the difference between our model and actual values.

Error Function used:

We have used the least square error function for our hypothesis.

$$J = (1/n) \sum (y - h(\boldsymbol{\theta}_x))^2 \quad (7)$$

We have used gradient descent algorithm to learn the value of $\boldsymbol{\theta}_0$ and $\boldsymbol{\theta}_1$ for our model.

- For equation between $\lambda_{\text{er},n}$ and E_f ,

$$\lambda_{\text{er},n} = \frac{W}{p} \sqrt{\left(\frac{2WE_f}{nh\nu_f} \right)^2 - 1} \quad (8)$$

We have assumed that $\lambda_{\text{er},n} = y$ and $E_f = x$ and taking other terms as constant and squared the equation on both sides. Through which we got $y^2 = b*(a*x^2 - 1)$. Since it is a polynomial equation, we used a polynomial regression model to learn the value of a and b . The hypothesis we have used is $h = b*(a*x^2 - 1)$ where our model is trained to learn the value of a and b .

How do we train our model ?

- We provide the values of E_f as x to our model and $\lambda_{\text{er},n}$ as y to our model.
- Model tries to learn the value of a and b .
- Model learns the value of a and b and uses it to predict the value of $\lambda_{\text{er},n}$.
- We plot the graph of $\lambda_{\text{er},n}$ vs E_f and then between $\lambda_{\text{er},n}$ predicted and E_f to know the difference between our model and actual values.

We have used the same error function in this model as well.

- For equation

$$\frac{1}{\lambda_{eff,n}} = \frac{1}{\lambda_d} + \frac{1}{\lambda_{pn}} + \frac{1}{\lambda_{er,n}} + \frac{1}{\lambda_{sr}} \quad (9)$$

We have used the same linear regression model as discussed above taking $1/\lambda_{er,n}=x$ and $1/\lambda_{eff,n}=y$ making the above equation as $y=m*x+c$.

- For equation between $\lambda_{er,n}$ and w ,

$$\lambda_{er,n} = \frac{W}{p} \sqrt{\left(\frac{2WE_f}{nh\nu_f}\right)^2 - 1} \quad (10)$$

We have used the same polynomial regression model as discussed above taking $\lambda_{er,n}=y$ and $w=x$ and squaring the equation making the equation as $y^2=a*x^4+b*x^2$ which is a polynomial equation.

Techniques used

Supervised Learning

In a *supervised* learning task, the data sample would contain a target attribute $\{y\}$ y , also known as *ground truth*. And the task is to learn a function F , that takes the non-target attributes X and outputs a value that approximates the target attribute, *i.e.* $F(X) \approx y$. The target attribute $\{y\}$ y serves as a teacher to guide the learning task, since it provides a benchmark on the results of learning. The data with a target attribute is called "*labeled*" data. Based on the above definition, for the task of predicting the given parameters with the labeled data, it can be told it is a supervised learning task. We have used two special cases of supervised learning :

1. **Linear Regression:-**Linear regression is a basic and commonly used type of predictive analysis. The overall idea of regression is to examine two things: (1) does a set of predictor variables do a good job in predicting an outcome (dependent) variable? (2) Which variables in particular are significant predictors of the outcome variable, and in what way do they—indicated by the magnitude and sign of the beta estimates—impact the outcome variable? These regression estimates are used to explain the relationship between one dependent variable and one or more independent variables. The simplest form of the regression equation with one dependent and one independent variable is defined by the formula $y = c +$

$m \cdot x$, where y = estimated dependent variable score, c = constant, m = regression coefficient, and x = score on the independent variable.

2. Polynomial Regression:-Polynomial regression is a form of regression analysis in which the relationship between the independent variable x and the dependent variable y is modelled as an n th degree polynomial in x . Polynomial regression fits a nonlinear relationship between the value of x and the corresponding conditional mean of y , denoted $E(y | x)$. Although polynomial regression fits a nonlinear model to the data, as a statistical estimation problem it is linear, in the sense that the regression function $E(y | x)$ is linear in the unknown parameters that are estimated from the data. For this reason, polynomial regression is considered to be a special case of multiple linear regression. It is defined by the formula:

$$y = a \cdot x^n + b \cdot x^{n-1} + \dots + k \cdot x^0$$

which is a polynomial equation of n^{th} degree.

Gradient Descent

We have used the technique of gradient descent for learning the various constants in our models. Gradient descent is a first-order iterative optimization algorithm for finding a local minimum of a differentiable function. The idea is to take repeated steps in the opposite direction of the gradient (or approximate gradient) of the function at the current point, because this is the direction of steepest descent. Conversely, stepping in the direction of the gradient will lead to a local maximum of that function; the procedure is then known as gradient ascent. It is an algorithm that finds the best-fit line for a given training dataset in a smaller number of iterations. If we plot m and c against MSE, it will acquire a bowl shape as shown below:

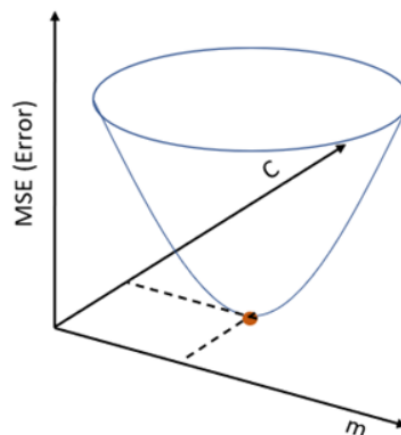


Fig.5.Gradient Descent

Testing details

- We have used python as a programming language to develop the machine learning models and to plot the data in graphical forms.
- We have used Origin software for creating graphs.
- We have developed the codes for all the formulas which requires the value of unknown variables to be put into .
- We use standard values of the constants used like Planck's constant.
- We trained our model on the generated data and then tested it on the same data further calculating the accuracy of our model.

Results and discussion:

- We created a linear regression model to predict the number of layers in GNR at a given thickness. In our model , Root mean squared error is 0.18648667982023368 and R score is 0.9999335602927097 which shows the accuracy of our model. The graph shown in Fig 6. Shows us that the number of layers increases as the thickness of GNR is increased.

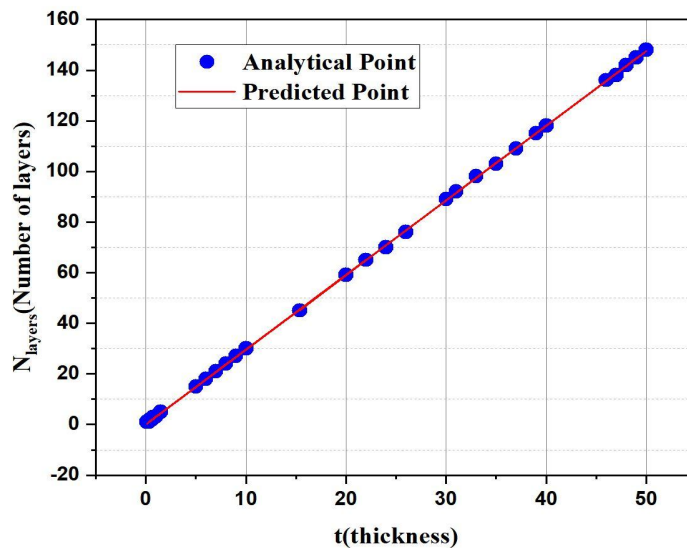


Fig.6.Number of layers dependency on the thickness of GNR

- We created a linear regression model to predict the number of channels in GNR at a given width and fixed value of fermi energy. In our model, we trained the model for three values of fermi energy which are 0.2eV, 0.4eV and 0.6eV. Root mean squared error is different for different values of fermi energy and R score is 0.9999916046297304 which shows the accuracy of our model. The graph shown in Fig 7. shows us that the number of channels increases as the width of GNR is

increased. It also indicates that more is the fermi energy, more will be the value of the number of channels at fixed width.

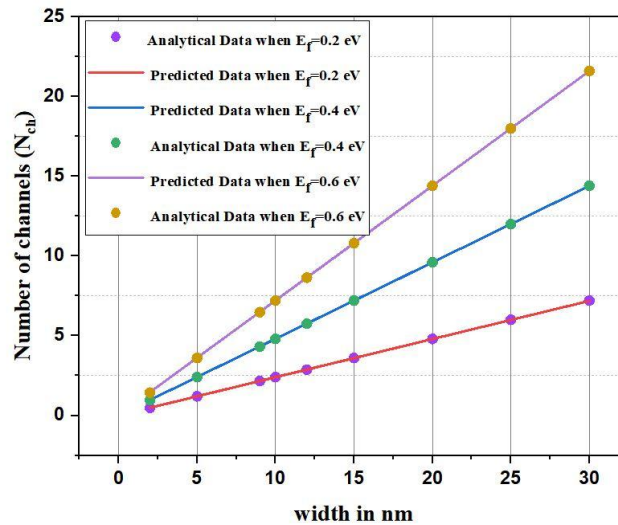


Fig.7.Dependency of number of channels on width at given E_f

- We created a linear regression model to predict the number of channels in GNR at a given fermi energy and fixed value of width. In our model, we trained the model for four values of width which are 7nm, 10nm, 13nm and 20nm. Root mean squared error is different for different values of width and R score is 0.9999763167516774 which shows the accuracy of our model. The graph shown in Fig 8. shows us that the number of channels increases as the fermi energy of GNR is increased. It also indicates that more is the width, more will be the value of the number of channels at fixed fermi energy.

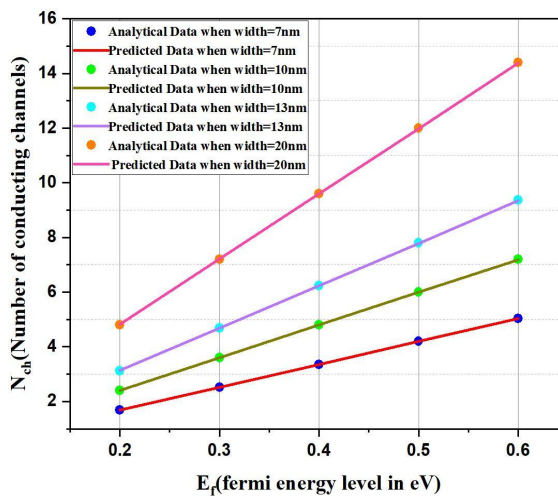


Fig.8..Dependency of number of channels on E_f at given width

- We created a combination of linear regression and polynomial regression models to predict the value of effective MFP for the nth sub-band $\lambda_{\text{eff},n}$ for the given values of fermi energy(E_f). The graph shown in Fig 9. shows us that the graph between $\lambda_{\text{eff},n}$ and E_f is hyperbolic in nature.

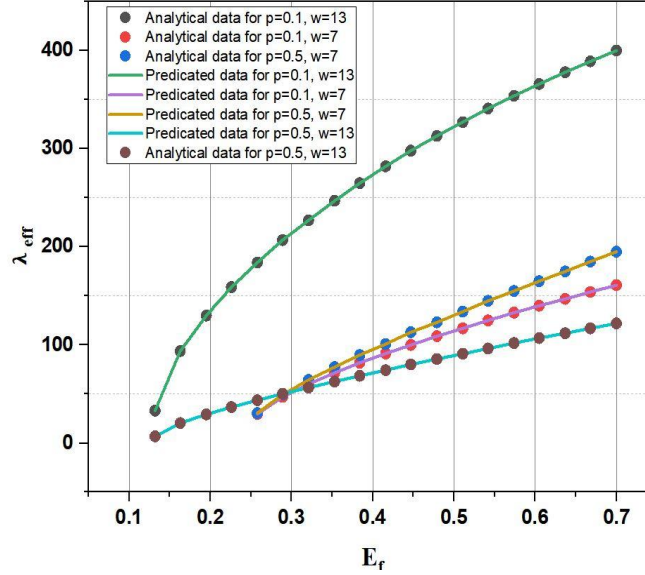


Fig.9.Dependency of effective MFP for the nth sub-band $\lambda_{\text{eff},n}$ on E_f at given values of p and w .

- We created a combination of linear regression and polynomial regression models to predict the value of effective MFP for the nth sub-band $\lambda_{\text{eff},n}$ for the given values of width in nm(w). The graph shown in Fig 10. shows us that the $\lambda_{\text{eff},n}$ increases with the decrease in fermi energy and with the decrease of p for the given value of width.

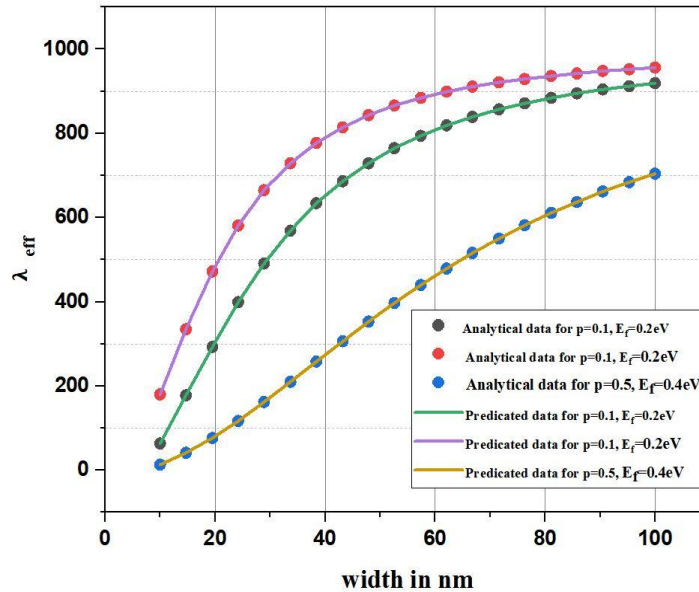


Fig.10.Dependency of effective MFP for the nth sub-band $\lambda_{\text{eff},n}$ on width(w) at given values of p and E_f .

- We created a combination of linear regression and polynomial regression models to predict the value of total resistance offered by the GNR at the given values of thickness. The graph shown in Fig 11. shows us that the resistance increases with the decrease in fermi energy and for the given value of thickness.

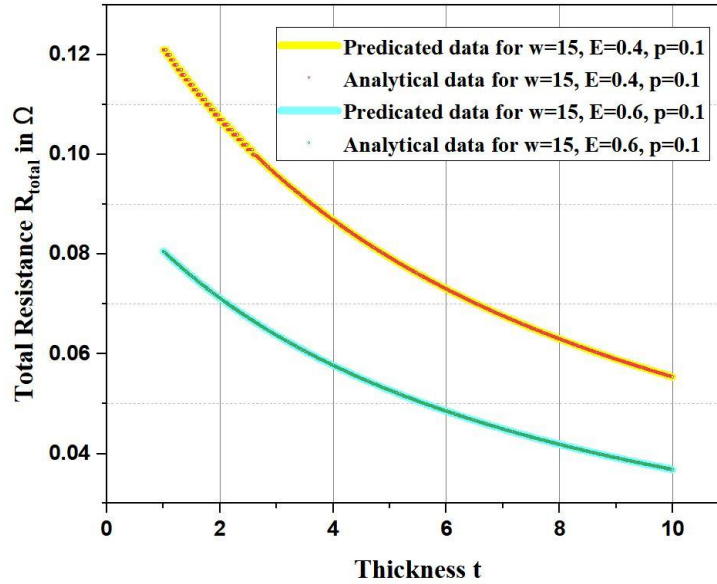


Fig.11.Dependency of total resistance on thickness (t) at given values of p, w and E_f .

- We created a combination of linear regression and polynomial regression models to predict the value of total resistance offered by the GNR at the given values of width in nm(w). The graph shown in Fig 12. shows us that the resistance is not much affected by the values of p and it is inversely proportional to the value of fermi energy.

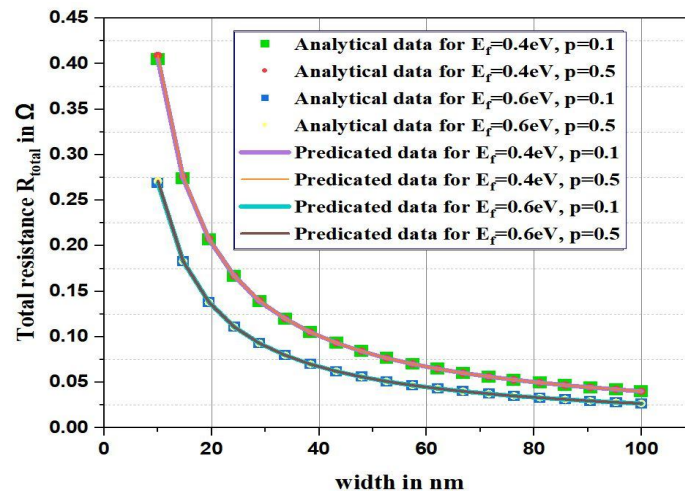


Fig.12.Dependency of total resistance on width (w) at given values of t, p and E_f .

Conclusion

We have concluded the following points from our research:

- Number of layers(N_{layer}) of GNR increases with increase in thickness of GNR with a similar proportion.
- Number of channels (N_{ch}) is directly proportional to the values of width(w) and fermi energy(E_f).
- The graph between $\lambda_{\text{eff},n}$ and E_f is hyperbolic in nature.
- Total resistance is increased by decreasing thickness to the same proportion.
- Total resistance is varying inversely to the width in nm.

Future Work

Resistance is the fundamental to many formulas related to capacitance , bandwidth , frequency , time delay and many more . We can use this model and expand it to predict the values of those parameters as well which are dependent on resistance , number of layers , MFP due to scattering , number of channels and effective MFP.

References :

- [1] "International technology roadmap for semiconductor," 2013. [Online].Available: <http://public.itrs.net>
- [2] S. Bothra, B. Rogers, M. Kellam, and C. Osburn, "Analysis of the effects of scaling on interconnect delay in ULSI circuits," IEEE Trans. Electron Devices, vol. 40, no. 3, pp. 591–597, Mar. 1993.
- [3] S. Im, N. Srivastava, K. Banerjee, and K. E. Goodson, "Scaling analysis of multilevel interconnect temperatures for high-performance ICs," IEEE Trans. Electron Devices, vol. 52, no. 12, pp. 2710–2719, Dec. 2005.
- [4] A. Naeemi and J. D. Meindl, "Performance modeling for single-and multiwall carbon nanotubes as signal and power interconnects in gigascale systems," IEEE Trans. Electron Devices, vol. 55, no. 10, pp. 2574–2582, Oct. 2008.
- [5] M. S. Sarto and A. Tamburrano, "Single-conductor transmission-line model of multiwall carbon nanotubes," IEEE Trans. Nanotechnol., vol. 9, no. 1, pp. 82–92, Jan. 2010.
- [6] M. D'amore, M. S. Sarto, and A. Tamburrano, "Fast transient analysis of next-generation interconnects based on carbon nanotubes," IEEE Trans. Electromagn. Compat., vol. 52, no. 2, pp. 496–503, May 2010.
- [7] W.-S. Zhao and W.-Y. Yin, "Comparative study on multilayer graphene nanoribbon (MLGNR) interconnects," IEEE Trans. Electromagn. Compat., vol. 56, no. 3, pp. 638–645, Jun. 2014.
- [8] V. R. Kumar, M. K. Majumder, N. R. Kukkam, and B. K. Kaushik, "Time and frequency domain analysis of MLGNR interconnects," IEEE Trans. Nanotechnol., vol. 14, no. 3, pp. 484–492, May 2015.
- [9] L. Qian, Y. Xia, and G. Shi, "Study of crosstalk effect on the propagation characteristics of coupled MLGNR interconnects," IEEE Trans. Nanotechnol., vol. 15, no. 5, pp. 810–819, Sep. 2016.
- [10] F. Liang, G. Wang, and H. Lin, "Modeling of crosstalk effects in multiwall carbon nanotube interconnects," IEEE Trans. Electromagn. Compat., vol. 54, no. 1, pp. 133–139, Feb. 2012.
- [11] A. Naeemi and J. D. Meindl, "Electron transport modeling for junctions of zigzag and armchair graphene nanoribbons (GNRs)," IEEE Electron Device Lett., vol. 29, no. 5, pp. 497–499, May 2008.
- [12] D. Gunlycke, H. Lawler, and C. White, "Room-temperature ballistic transport in narrow graphene strips," Phys. Rev. B, vol. 75, no. 8, 2007, Art. no. 085418.
- [13] G. Liang, N. Neophytou, D. E. Nikonov, and M. S. Lundstrom, "Performance projections for ballistic graphene nanoribbon field-effect transistors," IEEE Trans. Electron Devices, vol. 54, no. 4, pp. 677–682, Apr. 2007.

- [14] R. Murali, K. Brenner, Y. Yang, T. Beck, and J. D. Meindl, "Resistivity of graphene nanoribbon interconnects," *IEEE Electron Device Lett.*, vol. 30, no. 6, pp. 611–613, Jun. 2009.
- [15] T. Fang, A. Konar, H. Xing, and D. Jena, "Mobility in semiconducting graphene nanoribbons: Phonon, impurity, and edge roughness scattering," *Phys. Rev. B*, vol. 78, no. 20, 2008, Art. no. 205403.
- [16] A. Betti, G. Fiori, and G. Iannaccone, "Atomistic investigation of low-field mobility in graphene nanoribbons," *IEEE Trans. Electron Devices*, vol. 58, no. 9, pp. 2824–2830, Sep. 2011.
- [17] Y. Fang, W.-S. Zhao, X. Wang, F. Jiang, and W.-Y. Yin, "Circuit modelling of multilayer graphene nanoribbon (MLGNR) interconnects," in *Proc. Asia-Pac. Symp. Electromagn. Compat.*, Jul. 2012, pp. 625–628.
- [18] J.-P. Cui, W.-S. Zhao, W.-Y. Yin, and J. Hu, "Signal transmission analysis of multilayer graphene nano-ribbon (MLGNR) interconnects," *IEEE Trans. Electromagn. Compat.*, vol. 54, no. 1, pp. 126–132, Feb. 2012.
- [19] M. Dresselhaus and G. Dresselhaus, "Intercalation compounds of graphite," *Adv. Phys.*, vol. 30, no. 2, pp. 139–326, Jul. 1981.
- [20] M. Ishigami, J. Chen, W. Cullen, M. Fuhrer, and E. Williams, "Atomic structure of graphene on SiO₂," *Nano Lett.*, vol. 7, no. 6, pp. 1643–1648, 2007.
- [21] C. R. Dean et al., "Boron nitride substrates for high-quality graphene electronics," *Nature Nanotechnol.*, vol. 5, no. 10, pp. 722–726, 2010.
- [22] A. Zugarramurdi et al., "Determination of the geometric corrugation of graphene on SiC (0001) by grazing incidence fast atom diffraction," *Appl. Phys. Lett.*, vol. 106, no. 10, 2015, Art. no. 101902.
- [23] S. Babaee Touski and M. Pourfath, "Substrate surface corrugation effects on the electronic transport in graphene nanoribbons," *Appl. Phys. Lett.*, vol. 103, no. 14, 2013, Art. no. 143506.
- [24] M. Sanaeepur, A. Y. Goharizi, and M. J. Sharifi, "Performance analysis of graphene nanoribbon field effect transistors in the presence of surface roughness," *IEEE Trans. Electron Devices*, vol. 61, no. 4, pp. 1193–1198, Apr. 2014.
- [25] M. Sanaeepur, A. Y. Goharizi, and M. J. Sharifi, "Numerical investigation of the effect of substrate surface roughness on the performance of zigzag graphene nanoribbon field effect transistors symmetrically doped with BN," *Beilstein J. Nanotechnol.*, vol. 5, pp. 1569–1574, 2014.
- [26] A. Y. Goharizi, M. Sanaeepur, and M. Sharifi, "Improving performance of armchair graphene nanoribbon field effect transistors via boron nitride doping," *Superlattices Microstruct.*, vol. 85, pp. 522–529, 2015.
- [27] H. Raza and E. C. Kan, "Armchair graphene nanoribbons: Electronic structure and electric-field modulation," *Phys. Rev. B*, vol. 77, no. 24, 2008, Art. no. 245434.
- [28] Y.-W. Son, M. L. Cohen, and S. G. Louie, "Energy gaps in graphene nanoribbons," *Phys. Rev. Lett.*, vol. 97, no. 21, 2006, Art. no. 216803.
- [29] F. Ferranti, G. Antonini, T. Dhaene, L. Knockaert, and A. Orlandi, "Compact and accurate models of large single-wall carbon-nanotube interconnects," *IEEE Trans. Electromagn. Compat.*, vol. 53, no. 4, pp. 1025–1033, Nov. 2011.
- [30] C. Xu, H. Li, and K. Banerjee, "Modeling, analysis, and design of graphene nano-ribbon interconnects," *IEEE Trans. Electron Devices*, vol. 56, no. 8, pp. 1567–1578, Aug. 2009.
- [31] K. Nakada, M. Fujita, G. Dresselhaus, and M. S. Dresselhaus, "Edge state in graphene ribbons: Nanometer size effect and edge shape dependence," *Phys. Rev. B*, vol. 54, no. 24, 1996, Art. no. 17954.
- [32] A. Naemi and J. D. Meindl, "Compact physics-based circuit models for graphene nanoribbon interconnects," *IEEE Trans. Electron Devices*, vol. 56, no. 9, pp. 1822–1833, Sep. 2009.
- [33] V. Geringer et al., "Intrinsic and extrinsic corrugation of monolayer graphene deposited on SiO₂," *Phys. Rev. Lett.*, vol. 102, no. 7, 2009, Art. no. 076102.
- [34] H. Li, C. Xu, and K. Banerjee, "Carbon nanomaterials: The ideal interconnect technology for next-generation ICs," *IEEE Des. Test Comput.*, vol. 27, no. 4, pp. 20–31, Jul./Aug. 2010.
- [35] W. Y. Yin and W. S. Zhao, "Modeling of carbon nanotube (CNT) interconnects," in *Proc. IEEE Workshop SPI*, Naples, Italy, May 2011, pp. 79–82.
- [36] W. S. Zhao and W. Y. Yin, "Carbon-based interconnects for RF nanoelectronics," in *Wiley Encyclopedia of Electrical and Electronic Engineering*. New York, NY, USA: Wiley, Jul. 2012.
- [37] Semiconductor Industry Association, International Technology Roadmap for Semiconductors (ITRS), 2010 update, [Online]. Available: <http://www.itrs.net/>
- [38] R. Murali, Y. Yang, K. Brenner, T. Beck, and J. D. Meindl, "Breakdown current density of graphene nanoribbons," *Appl. Phys. Lett.*, vol. 94, no. 24, Jul. 2009.
- [39] H. Li, W. Y. Yin, K. Banerjee, and J. F. Mao, "Circuit modeling and performance analysis of multiwalled carbon nanotube interconnects," *IEEE Trans. Electron Devices*, vol. 55, no. 6, pp. 1328–1337, Jun. 2008.
- [40] A. Naemi and J. D. Meindl, "Performance modeling for single- and multiwall carbon nanotubes as signal and power interconnects in gigascale systems," *IEEE Trans. Electron Devices*, vol. 55, no. 10, pp. 2574–2582, Oct. 2008.
- [41] M. S. Sarto, A. Tamburrano, and M. D'Amore, "New electron-waveguide based modeling for carbon nanotube interconnects," *IEEE Trans. Nanotechnol.*, vol. 8, no. 2, pp. 214–215, Mar. 2009.
- [42] M. S. Sarto and A. Tamburrano, "Single-conductor transmission-line model of multiwall carbon nanotubes," *IEEE Trans. Nanotechnol.*, vol. 9, no. 14, pp. 82–92, Jan. 2010.

- [43] M. D'Amore, M. S. Sarto, and A. Tamburrano, "Fast transient analysis of next-generation interconnects based on carbon nanotubes," *IEEE Trans. Electromagn. Compat.*, vol. 53, no. 2, pp. 496–503, May 2010.
- [44] A. Maffucci, G. Miano, and F. Villone, "A new circuit model for carbon nanotube interconnects with diameter-dependent parameters," *IEEE Trans. Nanotechnol.*, vol. 8, no. 3, pp. 345–354, May 2009.
- [45] F. Ferranti, G. Antonini, T. Dhaene, L. Knockaert, and A. Orlandi, "Compact and accurate models of large single-wall carbon-nanotube interconnects," *IEEE Trans. Electromagn. Compat.*, vol. 53, no. 4, pp. 1025–1033, Nov. 2011.
- [46] I. S. Stievano, P. Manfredi, and F. G. Canavero, "Carbon nanotube interconnects: Process variation via polynomial chaos," *IEEE Trans. Electromagn. Compat.*, vol. 54, no. 1, pp. 140–148, Feb. 2012.
- [47] V. Kashcheyevs, A. Tamburrano, and M. S. Sarto, "Quantum transport and current distribution at ratio frequency in multiwall carbon nanotubes," *IEEE Trans. Nanotechnol.*, vol. 11, no. 3, pp. 492–500, May 2012.
- [48] S. N. Pu, W. Y. Yin, J. F. Mao, and Q. H. Liu, "Crosstalk prediction of single- and double-walled carbon-nanotube (SWCNT/DWCNT) bundle interconnects," *IEEE Trans. Electron Devices*, vol. 56, no. 4, pp. 560–568, Apr. 2009.
- [49] F. Liang, G. Wang, and H. Lin, "Modeling of crosstalk effects in multiwall carbon nanotube interconnects," *IEEE Trans. Electromagn. Compat.*, vol. 54, no. 1, pp. 133–139, Feb. 2012.
- [50] P. Avouris, "Graphene: Electronic and photonic properties and devices," *Nano Lett.*, vol. 10, no. 11, pp. 4285–4294, Sep. 2010.
- [51] A. Naeemi and J. D. Meindl, "Conductance modeling for graphene nanoribbon (GNR) interconnects," *IEEE Electron Device Lett.*, vol. 28, no. 5, pp. 428–431, May 2007.
- [52] A. Naeemi and J. D. Meindl, "Compact physics-based circuit models for graphene nanoribbon interconnects," *IEEE Trans. Electron Devices*, vol. 56, no. 9, pp. 1822–1833, Sep. 2009.
- [53] C. Xu, H. Li, and K. Banerjee, "Modeling, analysis, and design of graphene nano-ribbon interconnects," *IEEE Trans. Electron Devices*, vol. 56, no. 8, pp. 1567–1578, Aug. 2009.
- [54] M. S. Sarto and A. Tamburrano, "Comparative analysis of TL models for multilayer graphene nanoribbon and multiwall carbon nanotube interconnects," in *Proc. IEEE Int. Symp. Electromagn. Compat.*, Fort Lauderdale, FL, USA, Jul. 2010, pp. 212–217.
- [55] J. P. Cui, W. S. Zhao, W. Y. Yin, and J. Hu, "Signal transmission analysis of multilayer graphene nano-ribbon (MLGNR) interconnects," *IEEE Trans. Electromagn. Compat.*, vol. 54, no. 1, pp. 126–132, Feb. 2012.
- [56] Y. Sui and J. Appenzeller, "Screening and interlayer coupling in multilayer graphene field effect transistors," *Nano Lett.*, vol. 9, no. 8, pp. 2973–2977, 2009.
- [57] V. Kumar, S. Rakheja, and A. Naeemi, "Performance and energy-per-bit modeling of multilayer graphene nanoribbon conductors," *IEEE Trans. Electron Devices*, vol. 59, no. 10, pp. 2753–2761, Oct. 2012.
- [58] D. Das and H. Rahaman, "Crosstalk and gate oxide reliability analysis in graphene nanoribbon interconnects," in *Proc. Int. Symp. Electron. Syst. Des.*, Kochi, India, Dec. 2011, pp. 182–187.
- [59] C. Faugeras, A. Neri, M. Potemski, A. Mahmood, E. Dujardin, C. Berger, and W. A. de Heer, "Few-layer graphene on SiC, pyrolytic graphite, and graphene: A Raman scattering study," *Appl. Phys. Lett.*, vol. 92, no. 1, p. 011914, Jan. 2008.
- [60] A. Reina, X. Jia, J. Ho, D. Nezich, H. Son, V. Bulovic, M. S. Dresselhaus, and J. Kong, "Large area, few-layer graphene films on arbitrary substrates by chemical vapor deposition," *Nano Lett.*, vol. 9, no. 1, 2009.
- [61] M. Y. Han, B. Ozyilmaz, Y. Zhang, and P. Kim, "Energy band-gap engineering of graphene nanoribbons," *Phys. Rev. Lett.*, vol. 98, no. 20, p. 206805, May 2007.
- [62] D. Gunlycke, H. M. Lawler, and C. T. White, "Room-temperature ballistic transport in narrow graphene strips," *Phys. Rev. B, Condens. Matter*, vol. 75, no. 8, p. 085418, Feb. 2007.
- [63] Arizona State University, Predictive Technology Model (PTM), [Online]. Available: <http://www.eas.asu.edu/ptm/>
- [64] C. Berger, Z. Song, X. Li, X. Wu, N. Brown, C. Naud, D. Mayou, T. Li, J. Hass, A. N. Marchenkov, E. H. Conrad, P. N. First, and W. A. de Heer, "Electronic confinement and coherence in patterned epitaxial graphene," *Science*, vol. 312, no. 5777, p. 1191–1196, May 2006.
- [65] W. S. Zhao, W. Y. Yin, and Y. X. Guo, "Electromagnetic compatibility oriented study on through silicon single-walled carbon nanotube bundle via (TS-SWCNTBV) arrays," *IEEE Trans. Electromagn. Compat.*, vol. 54, no. 1, pp. 149–157, Feb. 2012.
- [66] H. Kempa, P. Esquinazi, and Y. Kopelevich, "Field-induced metal-insulator transition in the c-axis resistivity of graphite," *Phys. Rev. B*, vol. 65, p. 241101, May 2002.

